Physica A 468 (2017) 289–298

Contents lists available at ScienceDirect

Physica A

journal homepage: www.elsevier.com/locate/physa

# Hub-enhanced noise-sustained synchronization of an externally forced FitzHugh–Nagumo ring

Alejandro D. Sánchez *,[1], Gonzalo G. Izús [1], Matías G. dell'Erba [1], Roberto R. Deza

*IFIMAR (CONICET and Universidad Nacional de Mar del Plata), Deán Funes 3350, B7602AYL Mar del Plata, Argentina*

## HIGHLIGHTS

- Hub-enhanced noise-sustained synchronization of FHN cells is investigated.
- The whole system's dynamics is captured by a reduced few-cell model.
- Noise intensities for activation and synchronization are estimated.
- The model's results agree with the simulation ones.

## ARTICLE INFO

*Article history:*
Received 22 April 2016
Received in revised form 5 October 2016
Available online 3 November 2016

*Keywords:*
Synchronization
Complex systems
Noise in biological systems

## ABSTRACT

A ring of FitzHugh–Nagumo units with antiphase coupling between their activator fields and submitted to a adiabatic harmonic subthreshold signal, is in turn globally coupled in electrical mode with the activator field of a hub. Noise sustained synchronization of neural activity with the signal is numerically observed, and theoretically characterized. The different dynamical regimes are elucidated using the concept of nonequilibrium potential, and the hub is found to promote network synchronization. The minimum noise intensities triggering the activation and synchronization processes are estimated in the framework of a three-neuron model.



## 1. Introduction

In the theory of complex networks, hubs (highly connected nodes) are known to optimize the flow of information and orchestrate synchronization [1]. If the network is adaptive, it can critically self-organize into scale-free topology. For that reason, the existence of hub neurons in the cortex has long been conjectured. Until recently however [2], they had not been found in experiments.

Hub neurons are nowadays known to play a key role in brain function as a whole, for several reasons. On one hand, their high level of connectivity and their ability to link distant regions facilitates and accelerates the flow of information through the neural network [3]. On the other hand, they promote the synchronization of excitable neurons in the noisy environment of the cortex [4]. Synchronization is a crucial feature of neural networks, being it involved in a variety of cognitive functions (perceptual grouping, attention-dependent stimulus selection, routing of signals across distributed cortical networks, sensory-motor integration, working memory, and perceptual awareness [5]).

* Corresponding author.
*E-mail addresses:* sanchez@mdp.edu.ar (A.D. Sánchez), izus@mdp.edu.ar (G.G. Izús), mdellerba@ifimar-conicet.gob.ar (M.G. dellErba), deza@mdp.edu.ar (R.R. Deza).
[1] Member of CONICET, Argentina.

http://dx.doi.org/10.1016/j.physa.2016.10.096
0378-4371/

The organizing ability of hub neurons is highly efficient in terms of network functionality [6,7]: stimulation or inhibition of relatively few hub neurons triggers the activation of the neural network dynamics. As it is known however, perturbation of a single hub may affect the whole network dynamics. This becomes relatively fragile against the removal or abnormal maturation of some of these critical cells, leading to possible brain disorders as e.g. epilepsy, which is associated to disorder in network oscillations [8]. Therefore, understanding the neural network dynamics in the presence of hubs and characterizing its synchronization thresholds is of paramount importance. Note that even the dynamics of a single hub is not well studied, especially when the properties of nodes are not identical (recall that noise induces diversity). So studying such a piece of complex networks called "network motifs" [9,10] is fundamental to understand the phenomena in whole complex networks.

A highly effective model for numerically and analytically dealing with excitable behavior is the FitzHugh–Nagumo (FHN) one, a two-variable reduction of the celebrated Hodgkin–Huxley model. As excitable dynamics is stochastic in nature, a major theoretical development as the concept of nonequilibrium potential (NEP) [11,12] is certainly welcome. A NEP describing the excitable regime of the FHN model is not difficult to find [13,14] and can be exploited in complex situations, allowing e.g. to evaluate the noise intensity for synchronization as a function of some coupling strength.

While most of the existing works have focused on the noise effects in networks connected through global or local diffusive couplings, lesser attention has been paid to phase-repulsive coupling [15–18], where the cells tend to have a phase opposite to their nearest neighbors. Antiphase coupling plays an important role in circadian oscillation in the brain [19], synthetic genetic oscillators [20], the dynamics of astrocyte cultures [21], and has been used to investigate several aspects in the dynamics of neuronal and FHN coupled models [17,18,21–23] as well as Hodgkin–Huxley neurons [24,25]. In Refs. [26–31] we have considered a ring of FitzHugh–Nagumo units with antiphase coupling between their activator fields.

We now retrieve the model of Ref. [27] to study the effect of global coupling to a hub, on the noise-sustained synchronization between a ring of phase-repulsively coupled neurons and a subthreshold adiabatic external signal. In Section 2 we introduce the model, its dynamic equations and parameters. In Section 3 we provide numerical evidence of noise-sustained synchronization between the network and the external signal, and characterize the constructive role of noise in the process. In Section 4 we elucidate the observed dynamics in terms of the NEP of a reduced model. Finally, we collect our conclusions in Section 5. Appendix A devotes to estimating the noise intensity necessary to escape from a given state and Appendix B, to explain the deterministic growth of some numerically observed structures we call "antiphase states" (APS).

## 2. The model

The stochastic dynamics of the isolated cells is given by

$$\dot{u} = b\,u\,(1-u^2) - v + r_1\,\xi^{(u)}(t) + r_2\,\xi^{(v)}(t), \tag{1}$$

$$\dot{v} = \epsilon\,(\beta\,u - v + C) + r_3\,\xi^{(u)}(t) + r_4\,\xi^{(v)}(t), \tag{2}$$

where $u$ is the fast variable or *activator* (which mimics the action potential off the cell), and $v$ is the slow (recovery) variable or *inhibitor*, related to the time-dependent conductance of the $K^+$ channels in the membrane [32]. $\epsilon$ is the activator–inhibitor timescale ratio, and $C$ a tonic current. The $\xi^{(k)}$ ($k \in \{u, v\}$) are Gaussian white noises with intensity $\eta$: $\langle \xi^{(k)} \rangle = 0$ and $\langle \xi^{(k)}(t)\,\xi^{(l)}(t') \rangle = \eta\,\delta_{k,l}\,\delta(t-t')$. The values adopted throughout the work are: $\epsilon = 10^{-2}$, $\beta = 10^{-2}$, $b = 3.5 \times 10^{-2}$, $C = 2 \times 10^{-2}$, $\epsilon\,r_1 = r_3 = \cos 0.05$, and $\epsilon\,r_2 = r_4 = \sin 0.05$. Parameters $\epsilon$, $\beta$ and the $r$'s have been selected in such a way that they satisfy Eq. (13) below, an integrability condition required by the theoretical characterization of the dynamics.

The equations of the model are

$$\dot{u}_i = b\,u_i\,(1-u_i^2) - v_i + S(t) - D\,(u_{i+1} + u_{i-1}) + E\,(u_H - u_i) + r_1\,\xi_i^{(u)}(t) + r_2\,\xi_i^{(v)}(t), \tag{3}$$

$$\dot{v}_i = \epsilon\,(\beta\,u_i - v_i + C) + r_3\,\xi_i^{(u)}(t) + r_4\,\xi_i^{(v)}(t), \tag{4}$$

$$\dot{u}_H = b\,u_H\,(1-u_H^2) - v_H + \sum_{i=1}^{N} E\,(u_i - u_H) + r_1\,\xi_H^{(u)}(t) + r_2\,\xi_H^{(v)}(t), \tag{5}$$

$$\dot{v}_H = \epsilon\,(\beta\,u_H - v_H + C) + r_3\,\xi_H^{(u)}(t) + r_4\,\xi_H^{(v)}(t). \tag{6}$$

Subindices $i$ run from 1 to $N$, with $u_{N+1} \equiv u_1$ and $u_0 \equiv u_N$, and subindex $H$ labels the hub. $D$ and $E$ are the antiphase and electrical couplings, respectively. Noises applied to different cells are independent but have the same intensity $\eta$. Regarding the signal $S(t) = A_0 \sin \omega t$, $A_0$ and $\omega$ are low enough so that it can be regarded as subthreshold and adiabatic (the period remains above the typical deterministic time, i.e. the turnaround time of a single spike). Throughout the work, $A_0 = 1.1 \times 10^{-2}$, $\omega = 2 \times 10^{-3}$, $N = 256$ and $D = 10^{-2}$ have been adopted.

The central target of the paper is to investigate how affects the inclusion of an electrically coupled hub the synchronization processes of neuronal systems with the aptitude to develop noise-sustained synchronization. The choice of the underlying model (antiphase-coupled network without hub) is based on the robustness of its synchronization attractor.

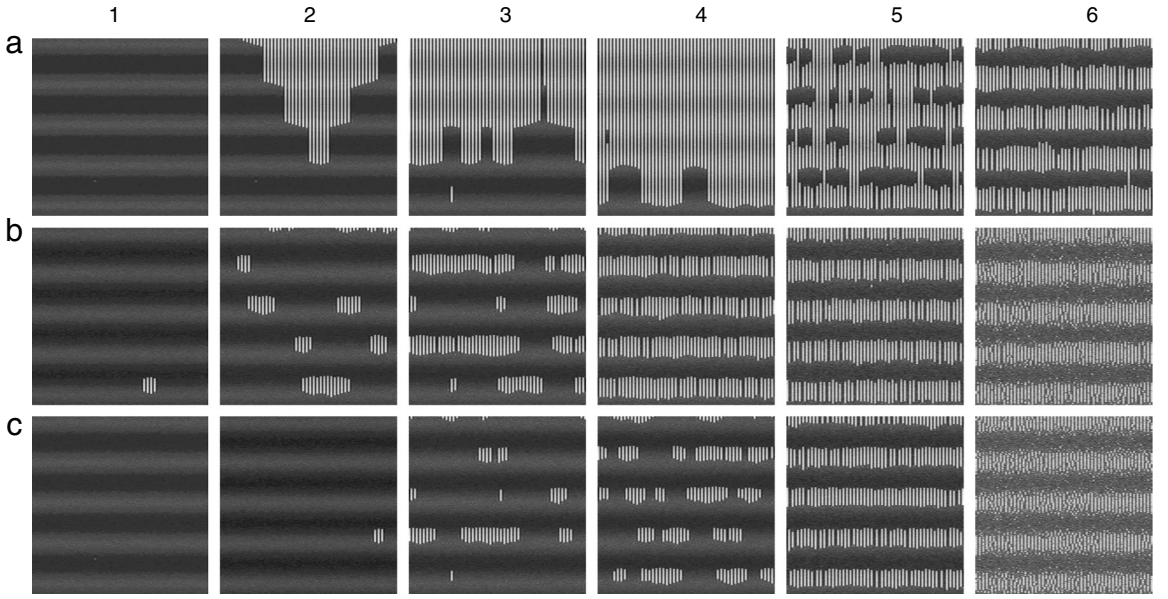


**Fig. 1.** Activity record of a subset of 100 neurons, during roughly four periods of the signal and the regimes summarized in Table 1. Light gray: activated cells; dark gray: inhibited cells. Horizontal axis denotes cells, vertical axis denotes time. Subthreshold oscillations, ring activation and synchronization can be observed, for example, in a1, a4 and a6 respectively.

**Table 1**
Coupling strengths and noise intensities corresponding to the frames in Fig. 1.

| Row | $E$ | $\eta$ | | | | | |
|---|---|---|---|---|---|---|---|
| a | $10^{-5}$ | $6 \times 10^{-9}$ | $8 \times 10^{-9}$ | $1.5 \times 10^{-8}$ | $2.7 \times 10^{-8}$ | $6.9 \times 10^{-8}$ | $1.405 \times 10^{-7}$ |
| b | $2 \times 10^{-3}$ | $1.5 \times 10^{-8}$ | $2.45 \times 10^{-8}$ | $3 \times 10^{-8}$ | $8.25 \times 10^{-8}$ | $3 \times 10^{-7}$ | $8 \times 10^{-7}$ |
| c | $4 \times 10^{-3}$ | $1.5 \times 10^{-8}$ | $2 \times 10^{-8}$ | $3.5 \times 10^{-8}$ | $4 \times 10^{-8}$ | $1.26 \times 10^{-7}$ | $9 \times 10^{-7}$ |

## 3. Noise sustained synchronization

A cell is said to be "activated" or "excited" whenever its activator field exceeds some threshold value $U_{\text{th}}$. The level of activity of the ring can be quantified by introducing the normalized global activity

$$A(t) = \frac{1}{N} \sum_{i=1}^{N} \Theta[u_i(t) - U_{\text{th}}], \tag{7}$$

where $\Theta$ is the Heaviside step function. As expected, $A(t)$ is not sensitive to $U_{\text{th}}$ within certain bounds. Hereafter we take $U_{\text{th}} = 0.4$. Since the antiphase coupling within the ring (controlled by $D$) tends to inhibit an excited neuron's nearest neighbors, spatially alternating states of excited and inhibited cells – which we call "antiphase states" (APS) [26–31] – are often observed. A perfect APS would yield $A = 0.5$. Activation is however a noise-assisted process, so alternance may fail due to the local noises and $A$ is unlikely to attain this value. Fig. 1 illustrates this point. The time evolution of the activator fields $u_i$ is shown for different values of the global coupling $E$ to the hub and different noise intensities $\eta$ (Table 1). The ordinate and abscissa axes in each frame stand respectively for time and the spatial order $i$ within a subset of the ring. The value of $u_i$ can be read off in gray scale, lighter cells being activated and darker ones inactive. Row (a) illustrates the formation (and eventual degradation) of the APS state (we call this mechanism *activation of the ring*) as $\eta$ increases, and further synchronization of the APS with the external signal. The other rows show synchronization without previous activation.

An indicator of the synchrony of the ring with the external signal $S(t)$ is the $Q$ factor, defined by

$$Q = \sqrt{Q_{\text{sin}}^2 + Q_{\text{cos}}^2}, \quad \text{with } Q_{\text{sin}} = \frac{2}{nT} \int_0^{nT} A(t) \sin(\omega t) \mathrm{d}t \quad \text{and} \quad Q_{\text{cos}} = \frac{2}{nT} \int_0^{nT} A(t) \cos(\omega t) \mathrm{d}t, \tag{8}$$

where $n$ is the number of periods $T$ covered by the integration time.

Fig. 2 plots the $Q$ factor as a function of the noise intensity $\eta$, for several values of $E$. The noise sustaining the dynamics has a *constructive* role for low intensities (it *enhances* coherence). As expected, this coherence degrades for larger noise intensities. In this regime we also observed that a larger global coupling to the hub requires larger noise intensities for optimal coherence. In the following we attempt to shed light on this scenario by resorting to the NEP formalism, which allows us to estimate the noise intensities for synchronization.

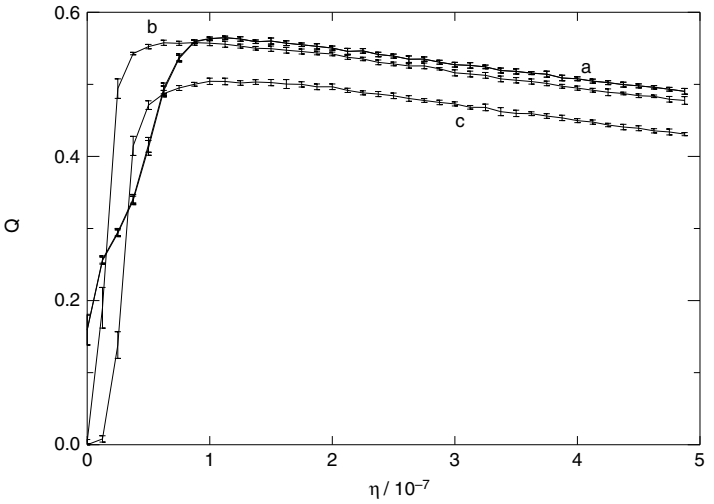


**Fig. 2.** $Q$ factor (average over 10 realizations) as a function of $\eta$: (a) $E = 0$ and $10^{-5}$ (virtually indistinguishable between them in the graph), (b) $1.35 \times 10^{-3}$, and (c) $4 \times 10^{-3}$.

## 4. Analytical approach to the problem

### 4.1. Nonequilibrium potential of the full model

For a system of Langevin-type equations, the nonequilibrium potential (NEP) $\Phi$ is defined through the zero-noise limit of the stationary probability density function $P$ by [11]

$$P = Z \exp\left[-\Phi/\eta + \mathcal{O}(\eta)\right]. \tag{9}$$

The NEP is a Lyapunov functional of the deterministic dynamics and provides information on the properties of attractors. In particular, it determines the height of the barriers separating attraction basins, which in turn define the transition rates among the different attractors.

For a general network of linearly coupled FitzHugh–Nagumo cells, the NEP has been derived in Ref. [28]. Applied to the present case, it reads

$$\Phi = \Phi_s(u_H, v_H) + \sum_{i=1}^{N}\left[\Phi_s(u_i, v_i) - \frac{2}{\lambda_1}S(t)\,u_i + \frac{2D}{\lambda_1}u_i u_{i+1} + \frac{E}{\lambda_1}(u_i - u_H)^2\right], \tag{10}$$

$$Z = \text{constant}, \tag{11}$$

$\Phi_s$ being the NEP for a single cell without signal,

$$\Phi_s(u, v) = \frac{\epsilon}{\lambda_2}(v^2 - 2\beta\, uv - 2Cv) + \frac{2\lambda\epsilon}{\lambda_1\lambda_2}(\beta\, u^2 + 2Cu) - \frac{2}{\lambda_1}\left[\frac{b}{2}u^2 - \frac{b}{4}u^4\right], \tag{12}$$

with $\lambda_1 = r_1^2 + r_2^2$, $\lambda_2 = r_3^2 + r_4^2$ and $\lambda = r_1 r_3 + r_2 r_4$. Integrability conditions (arising from the NEP's derivation) constrain the parameters to obey

$$\beta\lambda_1 + \lambda_2/\epsilon = 2\lambda. \tag{13}$$

The third term in Eq. (10) is the explicit contribution of the signal, the fourth one takes into account the antiphase coupling inside the network and the last one, the electrical coupling between the ring's neurons and the hub.

### 4.2. Reduced three-neuron model

A theoretical study of the dynamics can be done through the NEP. Given that in the APS each neuron in the ring is roughly in the same state as its second neighbor, we write the NEP as if all even neurons on one side and all odd ones on the other side were exactly in the same state, so that the whole ring is described by two neurons. Dividing the resulting NEP by $N/2$, we can interpret it as a simplified model where the ring is represented by a two-neuron system, and an additional neuron represents

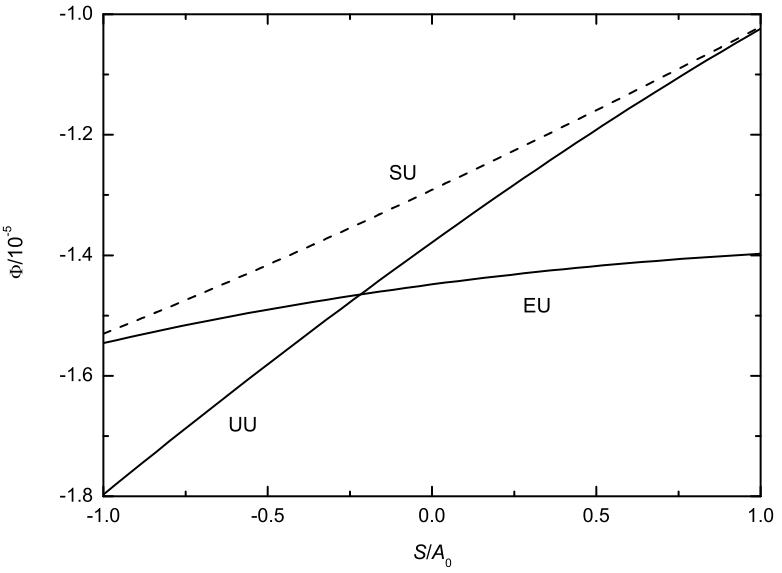


**Fig. 3.** NEP values at the minima (solid lines) and saddle (dashed line) of the three-neuron model, for $E = 10^{-5}$.

the hub. The two-neuron description of the ring (introduced in Ref. [27]) is the minimal description able to describe the APS. For the three-neuron model, the NEP in Eq. (10) takes the form

$$\Phi(u_1, v_1, u_2, v_2, u_H, v_H) = \Phi_s(u_1, v_1) + \Phi_s(u_2, v_2) + \frac{2}{N}\Phi_s(u_H, v_H) + \frac{1}{\lambda_1}\left\{-2S(u_1 + u_2) + 4D\,u_1u_2 + E\left[(u_1 - u_H)^2 + (u_2 - u_H)^2\right]\right\}. \quad (14)$$

The critical points of the NEP are identified by a two-letter code, which denotes the states of the two neurons representing the ring (the state of the hub needs not be denoted, since no NEP states differing *only* in the state of the hub have been found). An inhibited neuron is denoted by U and an activated one by E; if it is in an intermediate state, by S. Whenever at least one letter in the code is S, the corresponding critical point is a saddle point of the NEP. Due to the system's symmetry, two states whose two-letter codes differ by exchange are degenerate (they have the same NEP value). Thus except the UU state, all critical points are degenerate. Using this model, we analyze the different global behaviors of the system as the coupling strength $E$ is varied.

The noise intensity needed to escape with chance $p$ from a given state is estimated in Appendix A, Eq. (A.5), in terms of the barrier $\Phi_{\text{sad}}$ for whole system. Setting $\Phi_{\text{sad}} = (N/2)\,\Delta\Phi$, where $\Delta\Phi$ is the barrier for the reduced model, the noise intensity needed to escape with $p = 0.01$ chance is

$$\eta = \frac{\Delta\Phi}{2.3}. \quad (15)$$

The value of $p$ has been chosen small enough so that (being the barrier for return much higher than $\Delta\Phi$) one can safely assume that the system does not return to the original state once the transition occurs. This assumption greatly simplifies the calculation of the activation and synchronization onsets.

### 4.3. Weakly coupled hub

Fig. 3 illustrates the typical barrier structure occurring for small enough coupling strengths ($0 < E \leq 1.35 \times 10^{-3}$). There are five critical points over the entire $S$ range: UU plus two degenerate minima (UE and EU) and two degenerate saddles (SU and US). The dynamics consists of subthreshold oscillations – i.e. remaining in the UU state –, until the system can overcome the barrier and go to the EU state. For $E = 10^{-5}$ this occurs at $S = A_0$, with $\eta \approx 1.5 \times 10^{-8}$ (see a3 in Fig. 1). Since the barrier to escape from EU is larger that the first one, the system remains activated, namely in EU state. For a somewhat larger noise intensity ($\eta \approx 6.9 \times 10^{-8}$) it can even overcome the barrier at $S = -A_0$ and become synchronized (see a5 in Fig. 1). With this noise level the system thus alternates between UU and EU adiabatically follows the signal. Fig. 4 displays the activator field $u_H$ of the hub in the UU and EU state at $S = -A_0$ and $S = A_0$ respectively, as a function of the electric coupling $E$. The difference between both curves represents the excursion of the $u_H$ field at synchronization, with increasing amplitude as $E$ increases.

In simulations, activation begins as a local phenomenon because – as already reported [27] – it starts at individual cells rather than in the network as a whole (Fig. 1(a2)). In order to describe this phenomenon, we assume that if the noise intensity

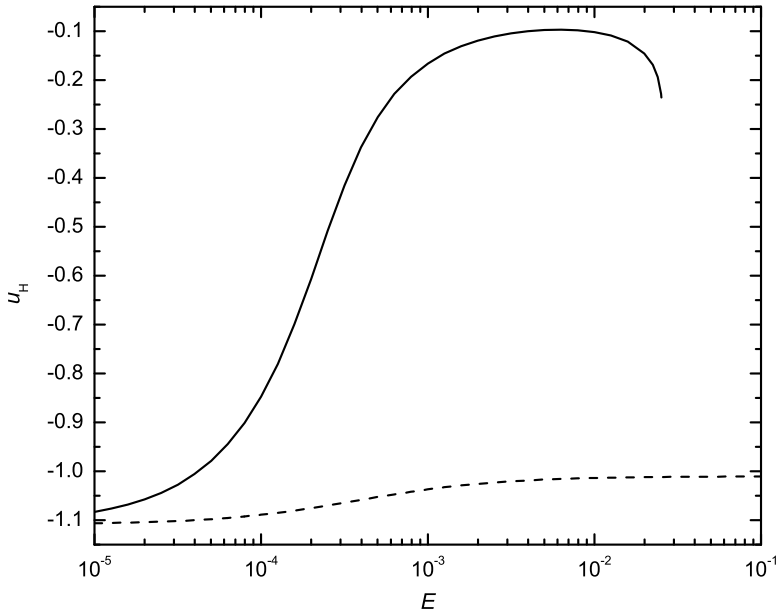


**Fig. 4.** Activator field $u_H$ of the hub, as a function of electric coupling $E$. Solid line: at the EU state (for $S = A_0$); dashed line: at the UU state (for $S = -A_0$). For each $E$ value, the difference between both curves yields the amplitude of the hub's oscillations in the synchronized regime, which has a maximum at $E \approx 5 \times 10^{-3}$.

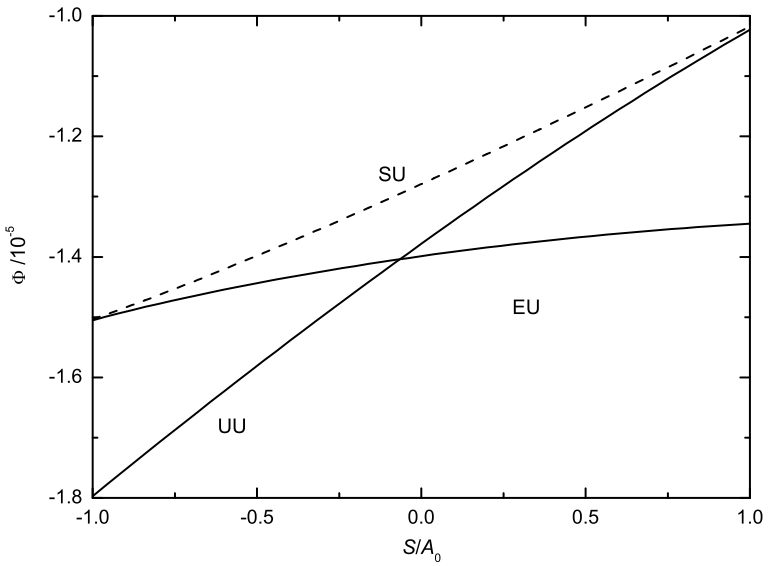


**Fig. 5.** NEP values in the minima (solid lines) and saddle (dashed line) of the three-neuron model, for $E = 2 \times 10^{-3}$.

is such that the activation probability of the whole network is 0.01, then 1% of its units will be locally activated (see details in Appendix A). For example, Fig. 1(a2) shows the evolution of a structure generated by the activation of a single neuron. Although the emergence of seeds is a stochastic process, their further growth is deterministic (as discussed in Appendix B). Note that in Fig. 1(a2), the seed does not appear until the second period of the signal has begun. This is consistent with the activation being less than 1% for that value of $\eta$.

### *4.4. Stronger hub–ring coupling*

For $1.36 \times 10^{-3} \leq E \leq 2.56 \times 10^{-3}$, although barrier structure is similar to the previous case to first glance, the first barrier (to escape from UU) is larger than the second one (to escape from EU), so there is no activation within this range of

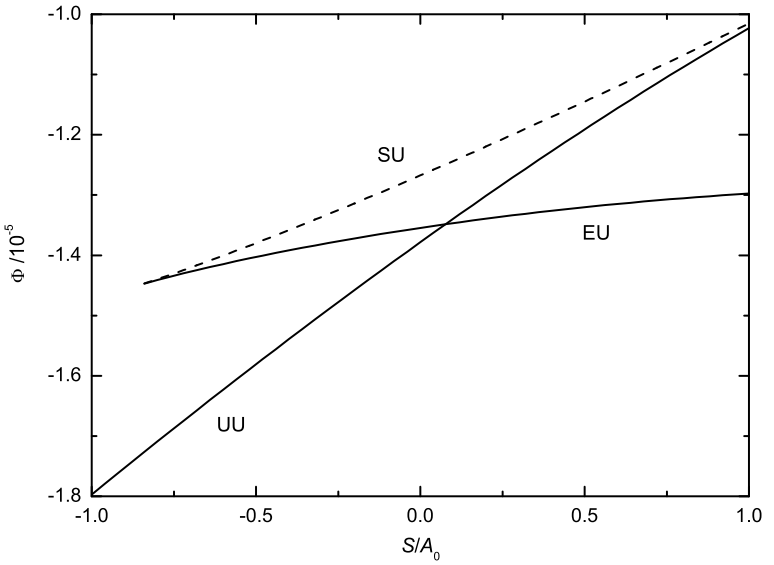


**Fig. 6.** NEP values in the minima (solid lines) and saddle (dashed line) of the three-neuron model, for $E = 4 \times 10^{-3}$.

values, and the system goes directly from subthreshold oscillations to synchronization. Fig. 5 shows the barrier structure for $E = 2 \times 10^{-3}$ as an example. For this coupling strength, the system performs subthreshold oscillations at small $\eta$ and synchronizes for larger $\eta$. The onset of synchronization is estimated to occur at $\eta = 2.45 \times 10^{-8}$ (see row b in Fig. 1).

For larger couplings ($2.57 \times 10^{-3} \leq E \leq 2.5 \times 10^{-2}$) the states SU and EU collapse for smaller signal values, and the second barrier disappears, but the dynamics remains similar to the previous case: the system passes from subthreshold oscillations to synchronization. Fig. 6 illustrates, as an example, the case for $E = 4 \times 10^{-3}$. The theoretical prediction for the onset of synchronization is $\eta \approx 3.5 \times 10^{-8}$ (see row c in Fig. 1).

For $E \geq 2.6 \times 10^{-2}$, only the UU state exists over the whole signal range. The curve of EU state in Fig. 4 ceases abruptly for higher values of $E$, because the EU (and SU) states do not exist anymore. As a consequence, activation and/or synchronization are not possible.

### 4.5. Dynamical regimes

Fig. 7 summarizes the different regions in the $\eta - E$ plane. The boundaries are calculated from the activation and synchronization barriers. The former are given by $\Phi(\mathrm{SU}) - \Phi(\mathrm{UU})$ at $S = A_0$ (for $0 < E \leq 1.35 \times 10^{-3}$); the latter, by $\Phi(\mathrm{SU}) - \Phi(\mathrm{EU})$ at $S = -A_0$ (for $0 < E \leq 1.35 \times 10^{-3}$) and $\Phi(\mathrm{SU}) - \Phi(\mathrm{UU})$ at $S = A_0$ (for $1.36 \times 10^{-3} \leq E \leq 2.5 \times 10^{-2}$).

We note that the hub promotes network synchronization. Fig. 7 shows that with respect to a network without hub (studied in Ref. [27] and corresponding to $E \to 0$ in Fig. 7), the noise intensity necessary to synchronize the network *decreases* until $E \approx 1.35 \times 10^{-3}$, and increases past this value. The reduction in $\eta$ at this optimal value of $E$ with regard to the $E = 0$ case is about 2.8 for the numerical data (maxima of the $Q$ factor) and 3.25 for the theoretical prediction (onset of synchronization).

## 5. Conclusions

In this paper we explore the effect of coupling globally (via electrical synapses) a network of FitzHugh–Nagumo neurons to an additional FitzHugh–Nagumo neuron, which acts as hub. The activator fields of the network's neurons are coupled in antiphase mode to those of their nearest neighbors, and are globally subject to a subthreshold harmonic external adiabatic signal. Moreover, each activator and inhibitor field is subject to independent white Gaussian noises of equal intensity.

The phenomena of activation and synchronization with the signal of the emergent antiphase structures were numerically studied. In particular, their dependence on the strength $E$ of the coupling to the hub. Simulations performed with increasing noise intensities revealed two routes toward synchronization:

1. For low $E$ there is a transition from subthreshold oscillations to activation of the ring, and then to synchronization with the signal (which finally degrades).
2. For larger $E$ values, there is no activation: by increasing the noise intensity, the transition occurs directly from subthreshold oscillations to network synchronization.

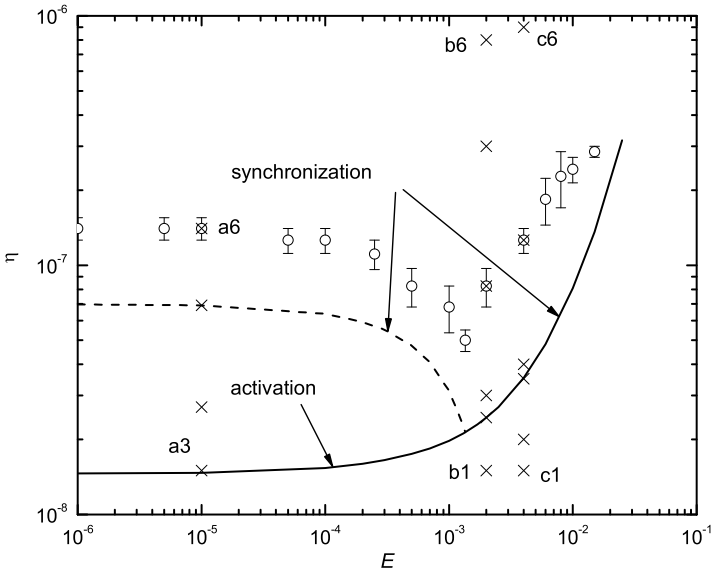


**Fig. 7.** Noise intensity vs. global coupling strength phase diagram, in log–log scale. The boundaries are determined from $\Phi(\mathrm{SU}) - \Phi(\mathrm{UU})$ at $S = A_0$ (solid line), and $\Phi(\mathrm{SU}) - \Phi(\mathrm{EU})$ at $S = -A_0$ (dashed line). The circles indicate the maxima of the $Q$ factor, obtained from simulations. The crosses locate the regimes corresponding to the snapshots in Fig. 1 (the labels are indicated, note that a1 and a2 lie outside the graph). For $E = 0$ the value of $\Delta\Phi$ for synchronization is $1.6 \times 10^{-7}$ (first calculated in Ref. [27]) that renders $\eta = 6.96 \times 10^{-8}$. For $E = 1.35 \times 10^{-3}$ (where both synchronization boundaries meet) $\eta = 2.14 \times 10^{-8}$.

The existence of a hub-enhanced synchronization mechanism is observed. This allows the ring to synchronize at lower noise levels that in the absence of the hub. The role of the noise is twofold: on one hand, it is (together with couplings and signal) an essential ingredient in this process; on the other, there is an optimal noise intensity for maximal coherence (the $Q$ factor exhibits a maximum as a function of the noise intensity).

Through a reduced three neuron model and using the concept of nonequilibrium potential (NEP), we obtain a signal-dependent potential landscape which explains the global dynamical regimes (in particular, both synchronization routes). This description is a simplified one, and of course do not take into account some system states which are present in numerical simulations, as for example the presence of defects (intended as the broke of periodicity in the cell states). Another fact that cannot be explained for the three neuron model is that simulations with relatively low noise show that the APS forms partially at the beginning, from nucleation seeds that grow deterministically at each period of the signal. This phenomenon could be explained through the NEP, using a model with a reduced number of variables (which greatly simplifies the theoretical treatment).

The barrier heights obtained in the framework of a three-neuron model, give an estimate of the noise intensities for the onset of activation and synchronization (it is worth noting that barriers for the whole system are exactly computed through the corresponding three-neuron model ones). The NEP provides a powerful framework to study the relationship between the architecture changes in the network (originated by the hub) and the effects induced by noise. In particular, the signal-dependent NEP landscape allows to quantify the levels of noise and to determine in each case which transitions are to be expected and which are not. We theoretically establish and numerically confirm that the noise threshold for synchronization has a minimum as a function of the global coupling $E$ with the hub. We also verify that the $Q$ factor is larger in this case than without hub. This result clearly shows that the inclusion of a single highly connected neuron improves the network's synchronization properties.

We remark that the noise-induced decays correspond to global decrease of the NEP, being the role of the signal to change adiabatically the relative stability between the wells, so providing the route to synchronization. This mechanism can be extrapolated to those systems for which an external signal induces a periodic change in the relative stability of the metastable attractors.

In conclusion, we have shown that NEP is a suitable tool to analyze deterministic and stochastic processes. Here we have focused on a case of great practical importance, which is the role of hubs in the synchronization process. We hope this methodology to work equally well in more realistic networks or systems.

## Acknowledgments

We acknowledge financial support from CONICET (project PIP 220100100315) and Universidad Nacional de Mar del Plata (project 15/E639), of Argentina.

## Appendix A. Noise intensity to escape from a state

Let $\mathbf{X}$ be the column vector whose $n = 2(N+1)$ components $x_i$ are the activator and inhibitor fields of the $N$ neurons in the ring plus those of the hub. Let us place the origin in the departure state $\alpha$ and take $\Phi = 0$ in this state. An expansion of $\Phi$ to second order in $\mathbf{X}$ yields

$$\Phi(\mathbf{X}) = \mathbf{X}^T A\, \mathbf{X}, \tag{A.1}$$

with $A_{ij} = \partial^2\Phi/(\partial_{x_i}\partial_{x_j})|_\alpha$ the Hessian matrix evaluated at $\alpha$. By the NEP's definition, Eq. (9), near state $\alpha$ we can approximate the stationary joint probability density function for $\mathbf{X}$ by

$$P(\mathbf{X}) = \frac{\sqrt{\det A}}{\pi^{n/2}}\, \exp\left(-\frac{\mathbf{X}^T A\, \mathbf{X}}{\eta}\right). \tag{A.2}$$

Hence the NEP's mean and standard deviation are $\langle\Phi\rangle = n\,\eta/2$ and $\sigma_\Phi := \sqrt{\langle\Phi^2\rangle - \langle\Phi\rangle^2} = \sqrt{n/2}\,\eta$, where $\langle f\rangle := \int_{-\infty}^{\infty} P(\mathbf{X})\, f(\mathbf{X})\, d^n x$. Note that Eq. (A.1) can we rewritten as

$$\Phi(\mathbf{X}) = \mathbf{X}'^T A'\, \mathbf{X}' = \sum_{i=1}^{n} A'_{ii} x'^2_i, \tag{A.3}$$

where $\mathbf{X}' = Q\mathbf{X}$, with $Q$ a orthogonal matrix such that $A' = Q^T A Q$ is a diagonal one. Since Eq. (A.3) is a linear combination of random variables with finite variance ($\chi^2$-distributed), we can (by invoking the Central Limit Theorem) approximate $P(\Phi)$ when the system is in state $\alpha$ by

$$P(\Phi) = \frac{1}{\eta\sqrt{\pi n}}\, \exp\left(-\frac{(\Phi - n\eta/2)^2}{n\eta^2}\right). \tag{A.4}$$

From Eq. (A.4) we get $\mathrm{Prob}(\Phi \geq \langle\Phi\rangle + \sigma_\Phi\, \delta) = p$, where $\delta = \sqrt{2}\,\mathrm{erfc}^{-1}(2p)$ and $\mathrm{erfc}^{-1}$ is the inverse complementary error function. In order to estimate escape from state $\alpha$ we adopt the criterion $\Phi_{\mathrm{sad}} = \langle\Phi\rangle + \sigma_\Phi\, \delta$, where $\Phi_{\mathrm{sad}}$ is the NEP value at the saddle point. Then, the noise intensities for the transition to occur with chance $p$ is

$$\eta = \frac{\Phi_{\mathrm{sad}}}{n/2 + \delta\sqrt{n/2}}. \tag{A.5}$$

## Appendix B. Deterministic growth from a single seed

In Fig. 1(a2) it is clearly seen that when partial activation takes place (i.e. for low $\eta$ values), it starts in a neuron and spreads to its neighbors. The three-neuron model being mean-field in nature, it cannot account for this phenomenon. In order to explain this process, we study a "partial activation model". To that end, we calculate the system's NEP when – except for five consecutive neurons of the ring – the values of the other activator fields are set to the value $U_l$ taken in the UU state of the three-neuron model. The hub's activator field will be fixed at $U_H$ (taken in the UU state of the three-neuron model), because only a small number of neurons can vary and being the hub connected to all the neurons, the hub field $u_H$ should not deviate much from $U_H$. Note that both $U_l$ and $U_H$ are functions of the signal's instantaneous value $S$. Thus, five consecutive neuron fields vary in this model. But since – due to the symmetry of the phenomenon – we set $u_1 = u_5$ and $u_2 = u_4$, there are only three variables. The NEP reads

$$\begin{aligned}\Phi(u_1, u_2, u_3) \;=\; & 2\Phi_s(u_1) + 2\Phi_s(u_2) + \Phi_s(u_3) - \frac{2}{\lambda_1} S(t)(2u_1 + 2u_2 + u_3) \\ & + \frac{4D}{\lambda_1}(U_l u_1 + u_1 u_2 + u_2 u_3) + \frac{E}{\lambda_1}[2(u_1 - U_H)^2 + 2(u_2 - U_H)^2 + (u_3 - U_H)^2],\end{aligned} \tag{B.1}$$

where we have omitted terms that not depending on $u_1$, $u_2$, or $u_3$ because they are irrelevant.

Fig. B.1 shows the NEP values at all the critical points of this model, for $E = 10^{-5}$. Although denoted by means of three letters, they correspond to 5 consecutive neurons. For example, the EUE state has three active neurons (separated by inhibited ones) on the uniform background.

For $S$ somewhat lower than $A_0$, being in the UUU state with a relatively low $\eta$, one can overcome the UUS barrier and reach the UUE state. But for $S = A_0$ there is no UUE state (it disappears by collapse with SUE, see details in the inset). Since the UUS saddle is still present, it continues to act as a barrier to escape from UUU. Although the system cannot end up anymore in UUE, it sweeps the region slowly and continues toward EUE. In other words, it starts with an excited neuron and deterministically ends up with three excited neurons. That is what is seen in the simulations: the APS area expands almost instantaneously and very neatly, which is consistent with it being deterministic. Obviously, the model does not allow the APS to expand farther than five neurons. But we have observed in similar models – differing only in their larger number of

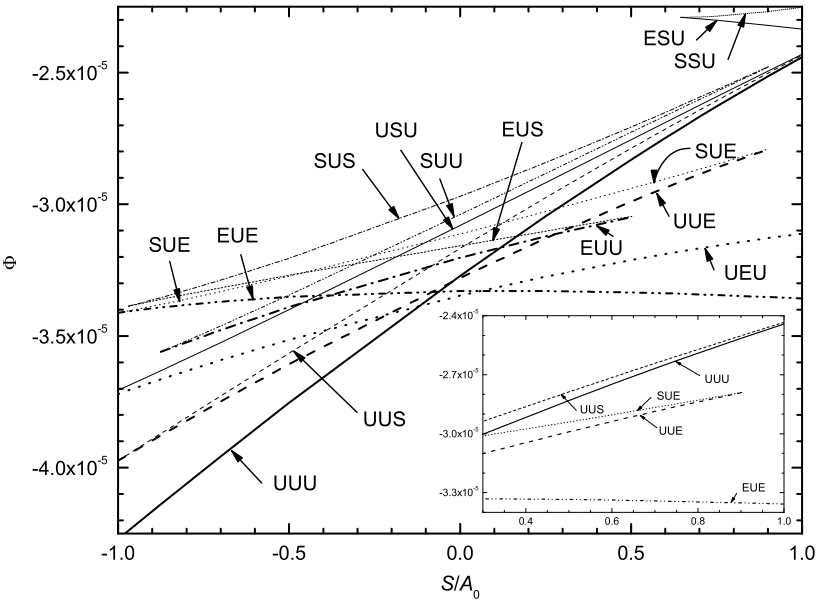


**Fig. B.1.** NEP value at the critical points for the partial activation model. Thick lines correspond to NEP minima, thin ones to saddles. The inset reproduces the most interesting portion of the graph (for clarity, some curves that are not relevant to explain the mechanism of deterministic growth have been removed).

variable neurons – that the states with three o more excited neurons disappear for larger signal values, just as it occurs with the state of an excited neuron in the model we are analyzing. As the signal value decreases during the time evolution, the APS which grew up to a certain number of neurons can no longer grow. However, it is stable for the attained configuration (i.e. it is a local minimum of the NEP). The system will deterministically escape in the next period of the signal (when this state will disappear) and the APS will continue to grow, as shown in Fig. 1(a2).

## References

[1] R. Albert, A.-L. Barabási, Rev. Modern Phys. 74 (2002) 47–97.
[2] P. Bonifazi, M. Goldin, M.A. Picardo, I. Jorquera, A. Cattani, G. Bianconi, A. Represa, Y. Ben-Ari, R. Cossart, Science 326 (2009) 1419–1424.
[3] O. Sporns, C.J. Honey, R. Kötter, PLoS One 2 (2007) e1049.
[4] L.M. Ward, Contemp. Phys. 52 (2009) 563.
[5] P.J. Uhlhaas, W. Singer, Neuron 52 (2006) 155.
[6] D. Malagarriga, A.E.P. Villa, J. García-Ojalvo, A.J. Pons, PLoS Comput. Biol. 11 (2015) e1004007.
[7] P. Massobrio, V. Pasquale, S. Martinoia, Sci. Rep. 5 (2015) 10578.
[8] R. Cossart, Curr. Opin. Neurobiol. 26 (2014) 51.
[9] R. Milo, S. Shen-Orr, S. Itzkovitz, N. Kashtan, D. Chklovskii, U. Alon, Science 298 (2002) 824–827.
[10] H. Kitajima, J. Kurths, Physica A 388 (2009) 4499–4508.
[11] R. Graham, in: E. Tirapegui, D. Villarroel (Eds.), Instabilities and Nonequilibrium Structures, D. Reidel, Dordrecht, 1987, pp. 271–290.
[12] H.S. Wio, R.R. Deza, Eur. Phys. J. Spec. Top. 146 (2007) 111.
[13] G.G. Izús, R.R. Deza, H.S. Wio, Phys. Rev. E 58 (1998) 93.
[14] G.G. Izús, R.R. Deza, H.S. Wio, Comput. Phys. Comm. 121–122 (1999) 406.
[15] S. Han, C. Kurrer, Y. Kuramoto, Phys. Rev. Lett. 75 (1995) 3190–3193.
[16] D. Postnov, S. Han, H. Kook, Phys. Rev. E 60 (1999) 2799–2807.
[17] E.I. Volkov, E. Ullner, J. Kurths, Chaos 15 (2005) 023105.
[18] C.J. Tessone, E. Ullner, A.A. Zaikin, J. Kurths, R. Toral, Phys. Rev. E 74 (2006) 046220.
[19] L. Yan, N. Foley, J. Bobula, L. Kriegsfeld, R. Silverl, J. Neurosci. 25 (2005) 9017–9026.
[20] E. Ullner, A. Zaikin, E. Volkov, J. García-Ojalvo, Phys. Rev. Lett. 99 (2007) 148103.
[21] G. Balázsy, A. Cornell-Bell, A. Neimal, F. Moss, Phys. Rev. E 64 (2001) 041912.
[22] A. Sherman, J. Rinzel, Proc. Natl. Acad. Sci. USA 89 (1992) 2471–2474.
[23] Q. Zhao, C. Yao, M. Yil, Eur. Phys. J. B 84 (2011) 299–305.
[24] Y. Li, G. Schmid, P. Hänggi, L. Schimansky-Geierl, Phys. Rev. E 82 (2010) 061907.
[25] X. Ao, G. Schmid, P. Hänggi, Math. Biosci. 245 (2013) 49–55.
[26] G.G. Izús, R.R. Deza, A.D. Sánchez, AIP Conf. Proc. 887 (2007) 89–95.
[27] G.G. Izús, A.D. Sánchez, R.R. Deza, Physica A 388 (2009) 967–976.
[28] A.D. Sánchez, G. Izús, Physica A 389 (2010) 1931–1944.
[29] M. dell'Erba, G. Cascallares, A.D. Sánchez, G. Izús, Eur. Phys. J. B 87 (2014) 82.
[30] A.D. Sánchez, G.G. Izús, M.G. dell'Erba, R.R. Deza, Phys. Lett. A 378 (2014) 1579–1583.
[31] G. Cascallares, A.D. Sánchez, M.G. dell'Erba, G. Izús, Physica A 433 (2015) 356–366.
[32] N.B. Janson, A. Balanov, E. Schöll, Phys. Rev. Lett. 93 (2004) 010601.